Test Beam characterization of a 180nm HV-CMOS pixel sensor

Francesca Maria Pofi, University of Rome La Sapienza, Italy

September 22, 2022

Abstract

As summer school project, a characterisation of the TelePix sensor under rotation around its x axis has been performed at the DESY II test beam facility. The goal was to study the influence of non perpendicular impact on the device performances.

The measurements have provided data to analyse the device performances under a rotation from 0 to 40 degrees and subject to different detection thresholds. The analysis performed for this work showed the angle in which the cluster size mean in row direction closest to two - 25 degrees - and the angle in which the highest amount of charge is collected in one pixel - 20 degrees.

From this information a more accurate reconstruction and analysis can be carried out to evaluate the performance of the sensor between these two angles, in particular the spatial resolution and the hit-detection efficiency.

Contents

1 Introduction

Beam telescopes are vital tools for R&D projects on particle detectors. Complementary to sensor simulations, test beam studies are used at various stages of chip development and are well suited for the performance evaluation of a detector prototype. To this end, a precise knowledge of 4D track information is needed. A pixelated sensor that provides both a precise time stamp and the spatial information allows for timing studies of devices under test (DUTs) the telescope. If the sensor is able to reject particles that travel outside the DUTs acceptance by a configurable region-of-interest (ROI) trigger output, it can also resolve the ambiguities created by data frame with multiple hits per sensor when the maximum available particle rate is used [1].
The test beam characterization on TelePix - a 180nm HV-CMOS pixel sensor- already shows promising result for the timing information and the ROI trigger.
In this work the spatial resolution is the subject of analysis: rotating the sensor to achieve higher charge sharing and reduced effective pitch is supposed to improve this. Measurements taken at the DESY II test beam facility from 22 August to 2 September varying both the angle between beam axis and sensor surface and the detection threshold applied are presented in the following sections.

2 DESY II Test Beam Facility & reference Telescope

2.1 DESY II Test Beam Facility

The generation of test beams starts in the DESY II synchrotron with a circumference of 292.8 m, that receives bunches of 10^{10} 0.45 GeV electrons or positrons from the linear accelerator LINAC II. The particles are then accelerated to typically 6.3 GeV, with a possible maximum of 7 GeV.
The test beams are generated by a double conversion instead of using a direct extraction. Initially a fiber target positioned in the DESY II beam orbit induces bremsstrahlung photons. These photons hit a secondary metal target generating electron/positron pairs. Depending on the polarity and strength of the magnetic field of a dipole magnet, electrons or positrons reaches the test beam areas with a certain momentum. Two collimators to select the momentum range and the particle rate follows. [4]
There are three independent beam lines -called TB21, TB22 and TB24- each one equipped with an EUDET-type Pixel Beam Telescope.
The TB21 beam line and an electron energy of 5 GeV were used for the measurements presented.

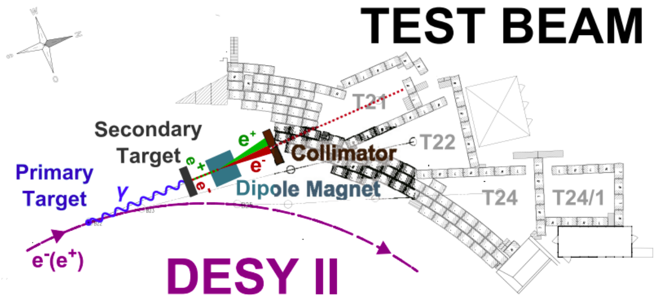

Figure 1: A schematic view of the test beam generation at the DESY II Test Beam Facility, here for beam line TB21.

2.2 Reference Telescope

Every EUDET-type beam telescope[5] is composed of two telescope arms each incorporating three planes. The standard telescope configuration has the DUT incorporated between three telescope planes upstream and three telescope planes downstream.
All the planes are equipped with a well-characterised pixel silicon sensor. In the reference telescope (Adenium) the ALPIDE chip[9] - designed for the Upgrade of the Inner Tracking System of the ALICE experiment at the CERN Large Hadron Collider - is used.
The ALPIDE is a Monolithic Active Pixel Sensor (MAPS) which is based on the 180 nm CMOS technology of TowerJazz. It measures 30 mm (X) by 15 mm (Y) and contains a matrix of 1024 x 512 sensitive pixels. The pixel pitch is 29.24μm x 26.88 μm and the binary resolution is improved by charge sharing up to 5μm x 5μm. The digital section includes three hit storage registers (Multi Event Buffer), a pixel masking register and pulsing logic. The front-end and the discriminator are continuously active.
To activate the telescopes' readout, the six planes are followed by a LySo scintillator. A Trigger Logic Unit (AIDA-TLU [2]) then generates a global clock signal and time reset in order to synchronise the Telescope and the Device Under Test (DUT): if the telescope planes receive a trigger from the TLU, the data is stored and a trigger ID is assigned to the read-out pixel hits, while the DUT DAQ receives a phase stable 125 MHz clock from the TLU and a reset signal at run start. The data acquisition for all devices is handled by the EUDAQ2 framework[7].

3 Device Under Test

The device under test is TelePix, a 180 nm HV-CMOS sensor that has been developed jointly by DESY, KIT and the University of Heidelberg and was designed at KIT.
The high-voltage technology allows combination of the standard low-voltage CMOS transistors - used to implement internal electronics of the chip - and the high-voltage devices used for fast output. To interface the two circuits a "floating logic" is used:

assuming a P-substrate process, all transistors are placed in a lowly doped deep N-well. The PMOS transistors are placed directly in the N-well, while the NMOS transistors are in the P-wells which are inside the deep N-well. The PN junction has lower dopant concentration than the one usually used in a CMOS process and can be biased with a reverse voltage up to 100V, inducing a depleted region larger than the standard CMOS one.[8] The substrate has a moderate resistivity (80-1000 Ohm). Signals are amplified with a PMOS transistor as the input device inside the active pixel and digitized in the periphery of the sensor. Both the time-of-arrival (ToA) and Time over-Threshold (ToT) are registered. It is possible to switch off the pixels individually. The chip operates trigger-less and continuously streams out data at 1.25 Gbit/s. Finally, TelePix uses a column-based readout architecture (column drain readout) without priority encoding and allows a fast and configurable Region Of Interest (ROI) trigger by selecting the pixel column range (HitBus option).

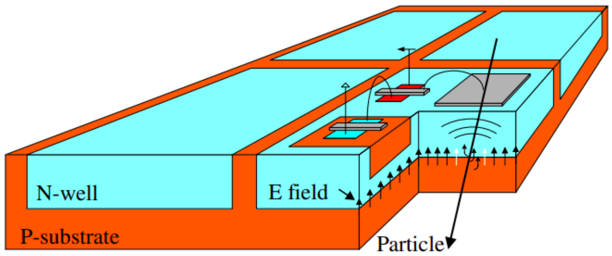

Figure 2: Sketch of four Telepix pixels

The device consists in a 29x124 matrix with a pixel pitch of 165 μm x 25 μm, for a total area of 4.8 mm x 3.1 mm. The thickness is 100 μm.
From previous Test-Beam characterisation[1] TelePix shows an hit detection efficiency of above 99.9 % at a bias voltage of -70 V, a time resolution of 3.16 ns. and delays of 32 ns at most with respect to the LySo trigger scintillator using the HitBus logic as a ROI trigger. In this characterisation a bias voltage of -70V is also used.

4 Performed Measurements

4.1 Rotation scans

The angle between beam axis and sensor surface was varied systematically to investigate the effect of oblique particle incidence. To this end, the DUT was mounted on a precision rotation stage and the distance between the telescope planes and DUT was increased to avoid the contact between the two for rotations up to 30 degrees, then a second shift was needed to allow the rotations up to 40 degrees. The device was rotated of 90 degrees to perform the angle variation around the local x axis, so in the direction in which it has the smaller pixel pitch.

Figure 3: Photo of the used setup: the DUT mounted on the rotation stage and incorporated by three telescope planes upstream and three telescope planes downstream stands out.

The position of the cluster associated to a track is calculated using a charge-weighted Centre-of-Gravity algorithm (CoG). The spatial residuals are given by the positional difference between the intercept of a track with the DUT and the associated cluster and the root mean square of this distribution is used to estimate on the spatial resolution of the DUT.
With increasing rotation angle, both the total energy deposition in the sensor due to the longer path in the active sensor region and the charge sharing due the energy deposition in several adjacent pixels increases. With more charge collected and more pixel hits for the same track, the CoG algorithm improves its performance and give a more precise cluster position reconstruction, resulting in smaller residuals and consequently a better spatial resolution.
The device was rotated from 0 to 40 degrees in steps of 5 degrees, then in steps of 1 degree around the angle with the cluster size closest to 2.

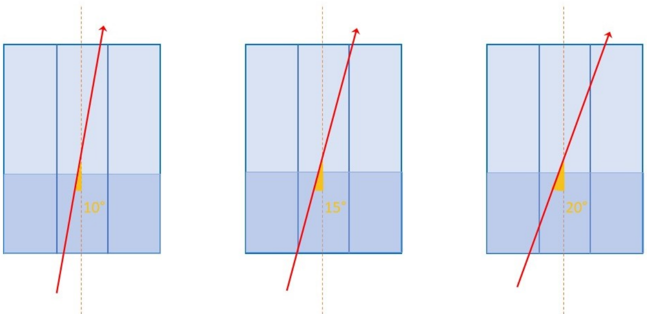

Figure 4: Sketch of the device's upper-view under rotation: after 14 degrees more than one pixel starts to be hit.

4.2 Threshold scans

The test-beam measurements for each angle were performed at various threshold values, allowing for an investigation of all performance parameters as a function of varying detection sensitivity.
When a particle pass through the sensor, a certain amount of electron-hole pairs are created, these charges are drifted by the electric field to the collection electrodes inducing a signal on them, which can be amplified and thus create a measurable electrical signal. If the signal is larger than the user-configurable threshold of the comparator, the traversing particle is detected as a hit.
With increasing rotation angle, the total energy deposition in the sensor increases due to the longer path in the active sensor region. As a result, a higher signal is detected, which would lead to an appreciable increase in efficiency at high thresholds.
The external applied detection threshold (in DAQ units) was initially changed from 159 to 259 in steps of 10, then the highest threshold applied was moved to 229. For some angles also a more accurate scan with steps of 5 was performed. The DAQ values 159-229 correspond approximately to 120-550 mV.

5 Test-Beam Reconstruction and Analysis

5.1 Corryvreckan

The analysis of test-beam data was performed with a dedicated software called Corryvreckan[3]. Corryvreckan is a framework based on a modular concept of the reconstruction chain: each step of the reconstruction is acted by a module - an user-configurable algorithm covering a specific task - and data objects are passed through them subsequently.

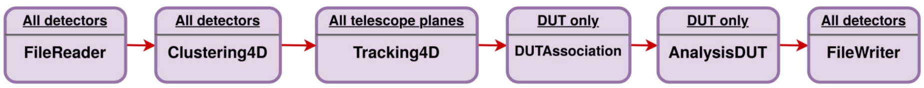

Figure 5: Example of reconstruction chain: each box represents a module

The main steps of the reconstruction chain are briefly reported.

- Reading Raw Data;
- Clustering: the algorithm needed to group adjacent pixels involved in the particle passage by charge sharing;
- Tracking: this algorithm combines clusters within a certain spatial and time interval on the planes of the reference telescope into a straight line, then a track

fitting algorithm is employed using an appropriate track model. In DESY II Test-Beam Facility the General Broken Line track fit[6] is chosen, to take in account the multiple scattering. The hits on the DUT are excluded in this step;

- Alignment: the algorithm that determine the precise x and y position of each plane with an iterative procedure. Three consecutive steps are performed: the prealignment, the telescope alignment and the DUT alignment. The shifts in the alignment stage minimise the track χ^2;
- Correlations: this algorithm calculates the spatial residuals between all detector planes and a reference plane cluster positions;
- DUT Association: a loop over all tracks to associate matching clusters on the DUT within a defined spatial and time interval is performed;
- Analysis DUT: it produces a number of commonly used plots to gauge detector performance and allows to discard tracks based on their χ^2/ndf value;
- Analysis Efficiency: this module measures the efficiency of the DUT by comparing its cluster positions with the interpolated track positions. It also provide a range of plots to investigate where inefficiencies might come from.

5.2 Main Parameters Analysed

From the Corryvreckan reconstruction four essential parameters are used to evaluate the performance of the DUT:

- **Cluster Size** is the number of pixels in a reconstructed cluster,this therefore serves as an observable to investigate charge-sharing properties. In the direction in which the device has the smaller pixel pitch more charge sharing is expected. For this reason the projection of the cluster onto the row direction is studied;
- **Pixel Time over-Threshold** is the signal pulse width at the selected detection threshold. It can be used as an estimate for the signal's charge collected in the device;
- **Residuals** are the differences between the position of the track intercept and the position of the associated cluster. The residuals are referred to as unbiased, since the DUT is excluded from the tracking to avoid biasing the measurement. An estimate of the spatial resolution of the DUT is given by the root mean square of this distribution;
- **Hit-detection Efficiency** is defined as the number of tracks associated to the DUT cluster over the total number of tracks. The tracks used for the hit-detection efficiency calculation are required to pass through the acceptance region of the DUT.

6 Results

The measurement results from two-week Test-Beam campaign from 22 August to 2 September at the DESY II Test-Beam Facility are reported.

6.1 Cluster Size

The cluster size - in particular the one in the tilt direction - is analyzed for each angle from 0 to 40. Figure 6 shows the two key results: the one in the left shows how the Cluster Size distribution changes with increasing the angle, in the plot on the right the behaviour of the mean cluster size under device rotation can be seen. The mean cluster size and so the charge-sharing increases non-linearly with the angle, due to the deposition of energy in multiple adjacent pixels. The angle with the cluster size nearer to 2 (two adjacent pixel hit) was found to be 25 degrees. That's in line with the expectations, because going over the 14 degrees two pixels starts to be crossed but initially the charge collected could not be enough to activate the second pixel. Also the depth of the depletion region can affect the cluster size.
The more precise scan changing the angle with steps of 1 degrees from 21 to 29 degrees reveal that the angle with the cluster size nearer to two is still 25.

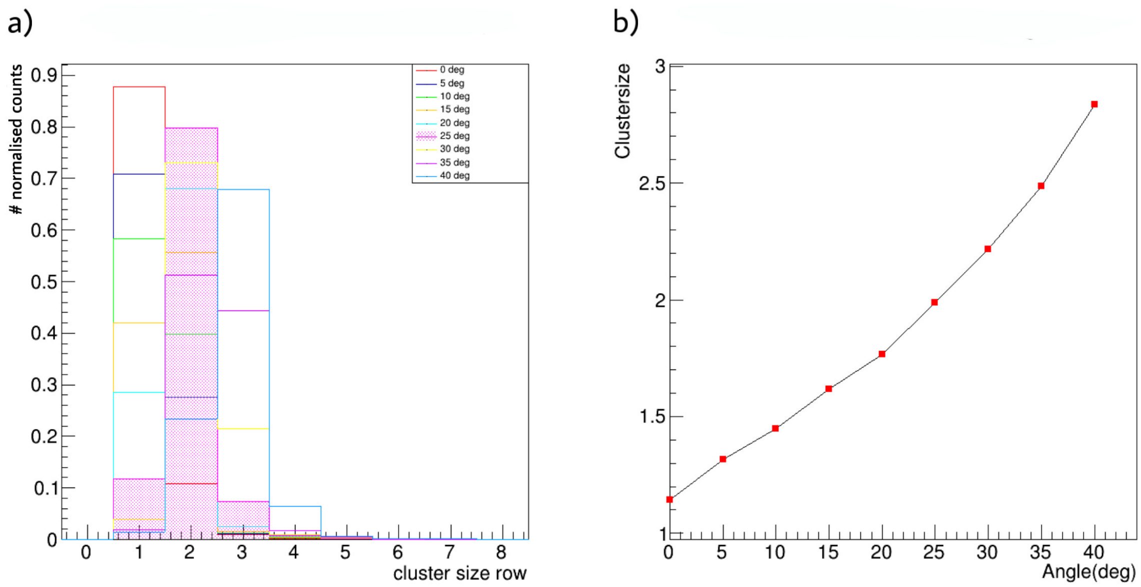

Figure 6: Number of associated clusters in row compared for the different device tilts performed from 0 to 40 degrees. In panel a): normalised cluster size distribution for all the device tilts performed. In panel b): mean cluster size against the rotation angle.

The cluster size is also highly sensitive to the detection threshold, since increasing the latter individual pixel signals can remain below the threshold, thus reducing the size of the cluster. The measurements agrees with the expected behaviour, as shown in the following plots computed on the threshold scan at 25 degrees: the cluster size exponentially decreases between the lower and the third threshold applied, then it reach a plateau around cluster size 1.

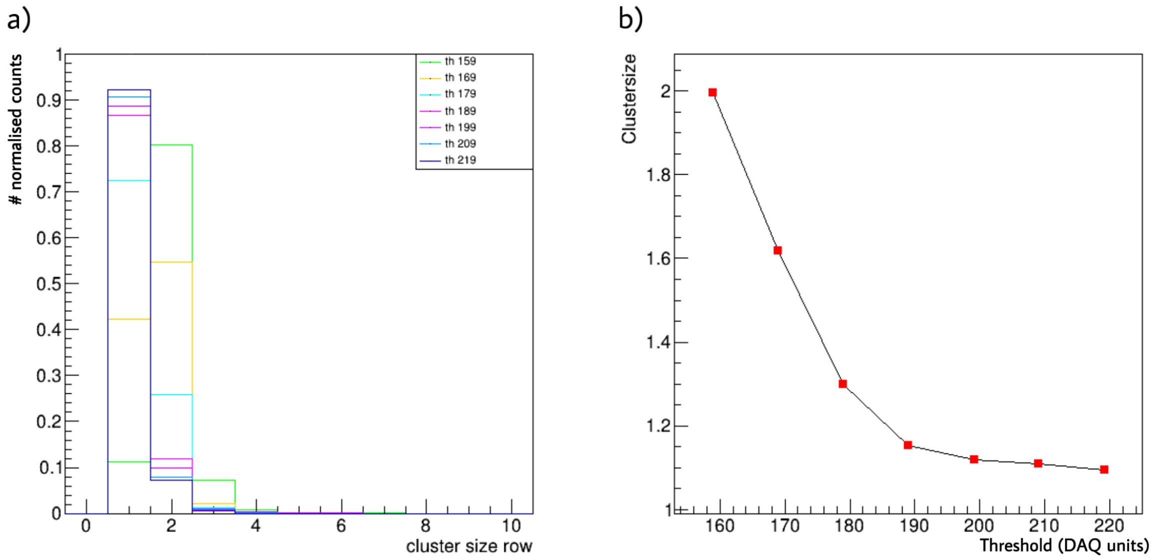

Figure 7: Number of associated clusters in row compared for the different threshold applied with a device tilt of 25 degrees. In panel a): normalised cluster size distribution for all the detection thresholds performed. In panel b): mean cluster size against the detection threshold.

6.2 Pixel Time over-Threshold

A first study on the pixel Time over-Threshold (ToT) is reported. To have a comparison of the ToT and so the charge collected in a single pixel, the mean values and the standard deviation given by ROOT statistics from the pixel ToT distributions are used. The estimate of the charge collected can be improved using a convolution between a Landau function an a polynomial one. We expect that the amount of charge collected increase with the tilt until it reaches a maximum, then decrease again going at longer angles. That's because after 14 degrees the charge carriers start to be created also in a third pixel, but in its undepleted region. Some of these carriers undergoes the recombination process so the amount charge collected result smaller, lowering the mean ToT.

As can be seen in Figure 8 the measurements' trend seems reasonable and show a maximum at 20 degrees. Despite that, the uncertainties are too huge to properly characterize the behaviour.

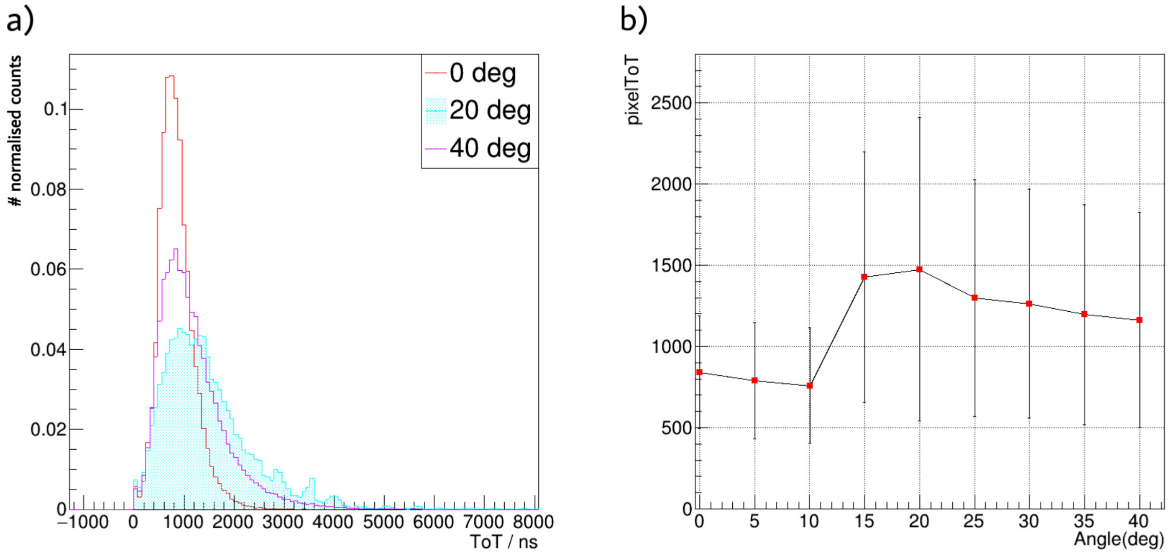

Figure 8: Time over-Threshold compared for the different device tilts performed from 0 to 40 degrees. In panel a): three selected normalised ToT distributions. In panel b): mean pixel ToT against the rotation angle.

7 Summary & Outlook

A characterisation of the TelePix sensor under rotation around its x axis has been performed at the DESY II test beam facility. The aim was to improve the spatial resolution in the row direction finding the tilt angle in which this parameter is the best one.
The measurements have provided data to analyse the device performances under a rotation from 0 to 40 degrees and subject to different detection thresholds. The analysis performed for this work showed the angle in which the cluster size mean in row direction closest to two - 25 degrees - and the angle in which the highest amount of charge is collected in one pixel - 20 degrees.
Starting from this information a more accurate reconstruction and analysis can be carried out to evaluate the performances between these two angles, in particular the spatial resolution and the hit-detection efficiency. To appreciate an improvement of the latter further alignment procedures should be done, as well as a correction for the non-linear charge sharing. Also a reconstruction taking into account the DUT in the Tracking algorithm could be done to calculate the biased residuals and have a more accurate esteem of the spatial resolution as $\sigma_{point} = \sqrt{\sigma_{biased} \cdot \sigma_{unbiased}}$.

8 Acknowledgements

I would like to thank my supervisor Lennart Huth for introducing me at the beamline and patiently explaining all the software used for analysis to me, the whole DESY-FH 65nm CMOS Pixel Detector Developments group for warmly incorporating me and all their time spent on giving first hands-on experiences and insights in the world of R&D on pixel sensors.
Moreover I would like to thank all my colleagues that enjoyed me at the test beam during the data taking: Judith, Sebastian, Giampiero and Arianna,TK.
I am also very grateful for the time spent with the other summer students: thanks for the trips, the coffees, the nights out, our talks, the pasta together, the advice, the biers, the complaints, the jokes. In particular, thanks to the italian summies: you've been like family to me.
Very special thanks are owed to the whole DESY Summer Student Program organisation team that made this unique opportunity possible.

References

[1] H. Augustin et al. "Upgrading the beam telescopes at the DESY II Test Beam Facility". In: *Nucl. Instrum. Meth. A* 1040 (2022), p. 167183. DOI: 10.1016/j.nima.2022.167183. arXiv: 2208.10827 [physics.ins-det].

[2] P. Baesso, D. Cussans, and J. Goldstein. "The AIDA-2020 TLU: a flexible trigger logic unit for test beam facilities". In: *Journal of Instrumentation* 14.09 (Sept. 2019), P09019–P09019. DOI: 10.1088/1748-0221/14/09/p09019. URL: https://doi.org/10.1088%5C%2F1748-0221%5C%2F14%5C%2F09%5C%2Fp09019.

[3] Dominik Dannheim et al. "Corryvreckan: A Modular 4D Track Reconstruction and Analysis Software for Test Beam Data". In: *JINST* 16.03 (2021), P03008. DOI: 10.1088/1748-0221/16/03/P03008. arXiv: 2011.12730 [physics.ins-det].

[4] R. Diener et al. "The DESY II Test Beam Facility". In: *Nucl. Instrum. Meth. A* 922 (2019), pp. 265–286. DOI: 10.1016/j.nima.2018.11.133. arXiv: 1807.09328 [physics.ins-det].

[5] Hendrik Jansen et al. "Performance of the EUDET-type beam telescopes". In: *EPJ Techniques and Instrumentation* 3 (Mar. 2016). DOI: 10.1140/epjti/s40485-016-0033-2.

[6] Claus Kleinwort. "General broken lines as advanced track fitting method". In: *Nuclear Instruments and Methods in Physics Research Section A: Accelerators, Spectrometers, Detectors and Associated Equipment* 673 (2012), pp. 107–110. ISSN: 0168-9002. DOI: https://doi.org/10.1016/j.nima.2012.01.024. URL: https://www.sciencedirect.com/science/article/pii/S0168900212000642.

[7] Y. Liu et al. "EUDAQ2—A flexible data acquisition software framework for common test beams". In: *JINST* 14.10 (2019), P10033. DOI: 10.1088/1748-0221/14/10/P10033. arXiv: 1907.10600 [physics.ins-det].

[8] Ivan Perić. "A novel monolithic pixelated particle detector implemented in high-voltage CMOS technology". In: *Nuclear Instruments and Methods in Physics Research Section A: Accelerators, Spectrometers, Detectors and Associated Equipment* 582.3 (2007). VERTEX 2006, pp. 876–885. ISSN: 0168-9002. DOI: https://doi.org/10.1016/j.nima.2007.07.115. URL: https://www.sciencedirect.com/science/article/pii/S0168900207015914.

[9] Valentina Raskina and Filip Křížek. "Characterization of Highly Irradiated ALPIDE Silicon Sensors". In: *Universe* 5.4 (2019). ISSN: 2218-1997. DOI: 10.3390/universe5040091. URL: https://www.mdpi.com/2218-1997/5/4/91.